

Supplemental Table 1: Radiopharmaceutical, special patient consideration, and dosimetry.

Radiopharmaceutical	Patient preparation	Special consideration	Administered Activity (intravenous)	Uptake time	Dosimetry
<sup>123</sup> I-MIBG	<p>Procedure guidelines (1). No fasting required.</p> <p>Thyroid blockade (2,3).</p> <p>Abstain from blocking medication that interfere with MIBG uptake (4-7)</p>	<p>Control hypertension/catecholamine excess: alpha +/- beta blockade (8). Beta blocker without alpha blockade should be avoided (9). Avoid certain drugs that can result in hypertensive crisis such as steroids or metoclopramide (the above are generally applicable consideration prior to any procedure).</p> <p>Patients often have prominent uptake in brown fat (10), not to be confused with lesions.</p>	<p>Adult weight base 80-370 MBq or Children: 5.2 MBq/kg with minimum of 20-37 MBq and maximum 370-400 MBq IV (1,11,12)</p>	<p>Typically , 24h planar/SP ECT-CT (1)</p>	<p>Effective dose equivalent 0.018mSv/MBq for adult and higher for children (13).</p>

<sup>18</sup> F-FDOPA	Procedure guidelines (14); Bozkurt, 2017 #38}. Fasting: 4h. No interfering medication.  Consider carbidopa pretreatment (15-17,18)		Adults or children: 2-4 MBq/kg typically 150 to 400 MBq IV in adults.	30-90min	The effective dose for adults is 0.025 mSv/MBq for adults and higher for children (19)
<sup>18</sup> F-FDG	Procedure guidelines generally applicable to PHEO/PGL (20). Patient are prone to hyperglycemia. Control glycemia prior to injection of FDG if possible.  Fasting overnight or at least 4-6h	Patients often have prominent uptake in brown fat (10), thus avoid cold temperature.	Adults: 2.5-5 MBq/kg, not to exceed 530 MBq IV(20). Pediatric weight-based (11).	Typically , 60 min	Adults receive 0.019 mSv/MBq effective dose with dose to children that are slightly higher per administered activity (19)
<sup>68</sup> Ga-DOTA-SSA	Procedure guidelines (21,22). No fasting required.	Stopping of somatostatin therapy, is recommended, prior to imaging or therapy. Recent studies suggest it may not to be necessary (23,24).	<sup>68</sup> Ga-DOTATATE 2 MBq/kg up to 200 MBq IV in adults.	60-90 min	Effective dose for <sup>68</sup> Ga-DOTATATE is 0.021 mSv/MBq and higher for children (package insert

				<p><a href="https://www.accessdata.fda.gov/drugsatfda_docs/label/2018/208547s011lbl.pdf">https://www.accessdata.fda.gov/drugsatfda_docs/label/2018/208547s011lbl.pdf</a> .</p> <p>Effective dose for <math>^{68}\text{Ga}</math>-DOTATOC is 0.021 mSv/MBq</p> <p><a href="https://www.accessdata.fda.gov/drugsatfda_docs/label/2019/210828s000lbl.pdf">https://www.accessdata.fda.gov/drugsatfda_docs/label/2019/210828s000lbl.pdf</a></p> <p>Effective dose for <math>^{64}\text{Cu}</math>-DOTATATE is 0.032 mSv/MBq</p> <p>(<a href="https://www.accessdata.fda.gov/drugsatfda_docs/label/2020/21322">https://www.accessdata.fda.gov/drugsatfda_docs/label/2020/21322</a>)</p>
--	--	--	--	---

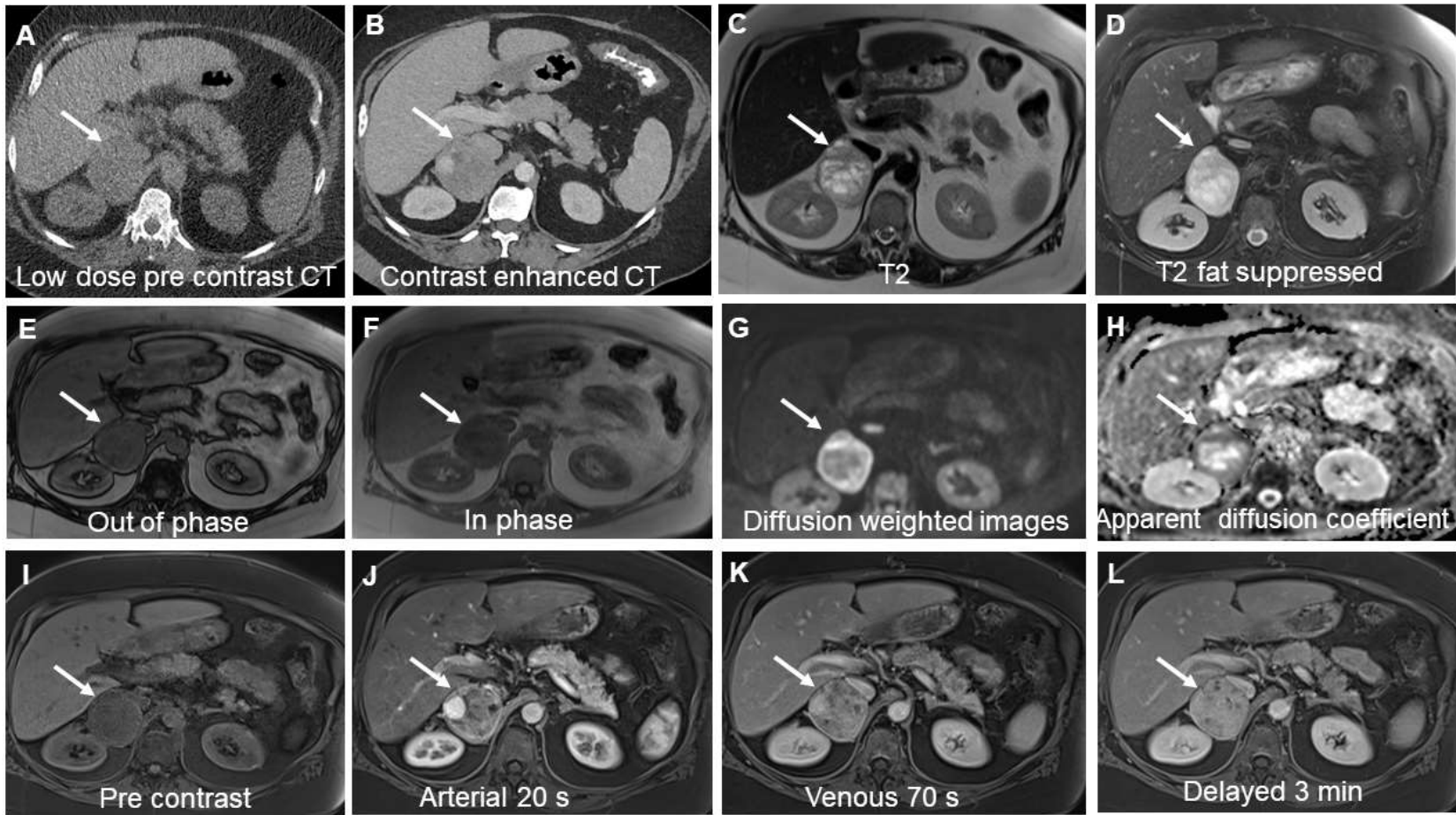
					7s0001b1.pdf)
--	--	--	--	--	---------------

Supplemental Table 2: Germline mutations, imaging sensitivity.

Gene	Relevant clinical presentation to imaging	<sup>123</sup> I-/ <sup>131</sup> I-MIBG	DOTA-SST	<sup>18</sup> F-FDG	<sup>18</sup> F-FDOPA
<i>RET</i>	MEN2: Predominantly PHEO, PGL are rare (25). Usually benign PHEO. Bilateral in 20-72% (26-29). Some develop other unrelated tumors. CT/MRI anatomical imaging is usually adequate in MEN2 patients with suspected PHEO.	80-100% sensitivity and lower specificity (30,31). Second choice for functional imaging.	100% <sup>68</sup> Ga-DOTANOC (30). Additional studies needed, preliminary study promising.	33% (31)	90%-100% sensitivity and high specificity (32,33). (34) Modality of choice when functional imaging is needed
<i>VHL</i>	Predominantly benign PHEO, with 2-5% malignant. 20% to 50% of PHEO occur bilaterally/multifocal (35-37). Some develop other unrelated tumors.	57%-78% (38,39). 40% of bilateral tumors detected (40)	Limited data	100% (39)	89-100% (41) (42,43)  Modality of choice

<i>MAX</i>	15.8% develop PGL, and 10.5% develop metastatic disease (44,45). Very small numbers imaged.	Limited data	57% <sup>68</sup> Ga-DOTATATE (46)	16% (46)	91% (46)  Modality of choice based on limited data
<i>NF1</i>	Neurofibromatosis 1, PHEO are more common than PGL (47); bilateral in 11.5%-20% (48-51); 7.3%-10% malignant disease (49,50).	50% (51)	Limited data	Limited data	100% (33,51)  Modality of choice
<i>EPAS 1 (HIF2 A) and EGLN 1</i>	Patients develop polycythemia, some also develop somatostatinoma and are associated with PHEO/PGL (52,53).	Limited data	35.3% for <sup>68</sup> Ga-DOTATATE, (54).	42.3% for <sup>18</sup> F-FDG (54).	98.7% (54).  <sup>18</sup> F-FDOPA is modality of choice

<p><i>SDHx</i></p>	<p>Variable phenotype depending on specific genotype. PGL more common than PHEO, some predominantly have HNPGL. Higher incidence of malignancy, specially <i>SDHB</i> and <i>SDHA</i>. (55-57).</p> <p>Imaging results for HNPGL ie predominantly SDHx related can be found in table 3.</p>	<p>43-65%, in metastatic (58-61)</p>	<p>94-99% in metastatic (62,63)          . Modality of choice</p>	<p>79-97%, in metastatic (58,60,62,63).</p> <p>Second choice for imaging</p>	<p>20%-61% in metastatic (60,62)</p>
--------------------	---	--------------------------------------	---	--	--------------------------------------



**Supplemental Figure 1. CT and MRI.** A 58-year-old female with a 6.0 cm right sporadic PHEO (arrows). (A) CT before contrast administration showing a right adrenal mass with radiodensity 36 HU (B) CT after contrast, portal venous phase. Mass is heterogeneous, with highest 131 HU, intermediate 71 HU, and lowest density 29 HU. (C) T2-weighted and (D) fat-suppressed T2-weighted images depict heterogeneity of mass, with T2-bright character most pronounced relative to normal anatomy in fat-suppressed image. (E) Out-of-phase and (F) in-phase images. There is no measurable signal loss in the out-of-phase images, implying a lipid-poor lesion. (G) Heavily diffusion-weighted and (H) apparent diffusion coefficient images. The bright area in the periphery of the mass in (G) corresponds to the less visually conspicuous dark periphery in (H), both indicating diffusion restriction in parts of the mass. (I) Pre-injection, and (J, 20 sec) early, (K, 70 sec) intermediate, and (L, 3 min) delayed post-injection fat-suppressed images demonstrating heterogeneity and typical intense early enhancement of a portion of the mass, which rapidly fades even as remaining portions of the mass gradually accrete contrast material over the 3 min post-injection interval.

## SUPPLEMENTARY TABLE REFERENCES:

1. Bombardieri E, Giammarile F, Aktolun C, et al. <sup>131</sup>I/<sup>123</sup>I-metaiodobenzylguanidine (mIBG) scintigraphy: procedure guidelines for tumour imaging. *Eur J Nucl Med Mol Imaging*. 2010;37:2436-2446.
2. Zanzonico PB, Becker DV. Effects of time of administration and dietary iodine levels on potassium iodide (KI) blockade of thyroid irradiation by I-131 from radioactive fallout. *Health Physics*. 2000;78:660-667.
3. Solanki KK, Bomanji JB, Waddington WA, Ell PJ, Committee UKAORSA. Thyroid blocking policy--revisited. *Nucl Med Commun*. 2004;25:1071-1076.
4. Babich JW, Graham W, Fischman AJ. Effect of adrenergic receptor ligands on metaiodobenzylguanidine uptake and storage in neuroblastoma cells. *Eur J Nucl Med*. 1997;24:538-543.
5. Jacobson AF, Travin MI. Impact of medications on mIBG uptake, with specific attention to the heart: Comprehensive review of the literature. *J Nucl Cardiol*. 2015;22:980-993.
6. Khafagi FA, Shapiro B, Fig LM, Mallette S, Sisson JC. Labetalol reduces iodine-131 MIBG uptake by pheochromocytoma and normal tissues. *J Nucl Med*. 1989;30:481-489.
7. Solanki KK, Bomanji J, Moyes J, Mather SJ, Trainer PJ, Britton KE. A pharmacological guide to medicines which interfere with the biodistribution of radiolabelled meta-iodobenzylguanidine (MIBG). *Nucl Med Commun*. 1992;13:513-521.
8. Pacak K. Preoperative management of the pheochromocytoma patient. *J Clin Endocrinol Metab*. 2007;92:4069-4079.
9. Luiz HV, Tanchee MJ, Pavlatou MG, et al. Are patients with hormonally functional pheochromocytoma and paraganglioma initially receiving a proper adrenoceptor blockade? A retrospective cohort study. *Clin Endocrinol (Oxf)*. 2016;85:62-69.
10. Hadi M, Chen CC, Whatley M, Pacak K, Carrasquillo JA. Brown fat imaging with (18)F-6-fluorodopamine PET/CT, (18)F-FDG PET/CT, and (123)I-MIBG SPECT: a study of patients being evaluated for pheochromocytoma. *J Nucl Med*. 2007;48:1077-1083.
11. Lassmann M, Biassoni L, Monsieurs M, Franzius C, Dosimetry E, Paediatrics C. The new EANM paediatric dosage card: additional notes with respect to F-18. *Eur J Nucl Med Mol Imaging*. 2008;35:1666-1668.
12. Bar-Sever Z, Biassoni L, Shulkin B, et al. Guidelines on nuclear medicine imaging in neuroblastoma. *Eur J Nucl Med Mol Imaging*. 2018;45:2009-2024.
13. ICRP. Radiation dose to patients from radiopharmaceuticals. A report of a Task Group of Committee 2 of the International Commission on Radiological Protection. *Ann ICRP*. 1987;18:1-377.
14. Taieb D, Hicks RJ, Hindie E, et al. European Association of Nuclear Medicine Practice Guideline/Society of Nuclear Medicine and Molecular Imaging Procedure Standard 2019 for radionuclide imaging of pheochromocytoma and paraganglioma. *Eur J Nucl Med Mol Imaging*. 2019;46:2112-2137.

15. Brown WD, Oakes TR, DeJesus OT, et al. Fluorine-18-fluoro-L-DOPA dosimetry with carbidopa pretreatment. *J Nucl Med.* 1998;39:1884-1891.
16. Hoffman JM, Melega WP, Hawk TC, et al. The effects of carbidopa administration on 6-[18F]fluoro-L-dopa kinetics in positron emission tomography. *J Nucl Med.* 1992;33:1472-1477.
17. Orlefors H, Sundin A, Lu L, et al. Carbidopa pretreatment improves image interpretation and visualisation of carcinoid tumours with 11C-5-hydroxytryptophan positron emission tomography. *Eur J Nucl Med Mol Imaging.* 2006;33:60-65.
18. Timmers HJ, Hadi M, Carrasquillo JA, et al. The effects of carbidopa on uptake of 6-18F-Fluoro-L-DOPA in PET of pheochromocytoma and extraadrenal abdominal paraganglioma. *J Nucl Med.* 2007;48:1599-1606.
19. Icrp. Radiation dose to patients from radiopharmaceuticals. Addendum 3 to ICRP Publication 53. ICRP Publication 106. Approved by the Commission in October 2007. *Ann ICRP.* 2008;38:1-197.
20. Boellaard R, O'Doherty MJ, Weber WA, et al. FDG PET and PET/CT: EANM procedure guidelines for tumour PET imaging: version 1.0. *Eur J Nucl Med Mol Imaging.* 2010;37:181-200.
21. Bozkurt MF, Virgolini I, Balogova S, et al. Guideline for PET/CT imaging of neuroendocrine neoplasms with (68)Ga-DOTA-conjugated somatostatin receptor targeting peptides and (18)F-DOPA. *Eur J Nucl Med Mol Imaging.* 2017;44:1588-1601.
22. Virgolini I, Ambrosini V, Bomanji JB, et al. Procedure guidelines for PET/CT tumour imaging with 68Ga-DOTA-conjugated peptides: 68Ga-DOTA-TOC, 68Ga-DOTA-NOC, 68Ga-DOTA-TATE. *Eur J Nucl Med Mol Imaging.* 2010;37:2004-2010.
23. Aalbersberg EA, de Wit-van der Veen BJ, Versleijen MWJ, et al. Influence of lanreotide on uptake of (68)Ga-DOTATATE in patients with neuroendocrine tumours: a prospective intra-patient evaluation. *Eur J Nucl Med Mol Imaging.* 2019;46:696-703.
24. Ayati N, Lee ST, Zakavi R, et al. Long-Acting Somatostatin Analog Therapy Differentially Alters (68)Ga-DOTATATE Uptake in Normal Tissues Compared with Primary Tumors and Metastatic Lesions. *J Nucl Med.* 2018;59:223-227.
25. Rodriguez JM, Balsalobre M, Ponce JL, et al. Pheochromocytoma in MEN 2A syndrome. Study of 54 patients. *World J Surg.* 2008;32:2520-2526.
26. Mannelli M, Castellano M, Schiavi F, et al. Clinically guided genetic screening in a large cohort of italian patients with pheochromocytomas and/or functional or nonfunctional paragangliomas. *J Clin Endocrinol Metab.* 2009;94:1541-1547.
27. Jansson S, Khorram-Manesh A, Nilsson O, et al. Treatment of bilateral pheochromocytoma and adrenal medullary hyperplasia. In: Pacak K, Eisenhofer G, eds. *Pheochromocytoma.* Vol 1073; 2006:429-435.
28. Thosani S, Ayala-Ramirez M, Palmer L, et al. The characterization of pheochromocytoma and its impact on overall survival in multiple endocrine neoplasia type 2. *J Clin Endocrinol Metab.* 2013;98:E1813-1819.

29. Waguespack SG, Rich T, Grubbs E, et al. A current review of the etiology, diagnosis, and treatment of pediatric pheochromocytoma and paraganglioma. *J Clin Endocrinol Metab.* 2010;95:2023-2037.
30. Sharma P, Dhull VS, Arora S, et al. Diagnostic accuracy of (68)Ga-DOTANOC PET/CT imaging in pheochromocytoma. *Eur J Nucl Med Mol Imaging.* 2014;41:494-504.
31. Timmers HJ, Chen CC, Carrasquillo JA, et al. Staging and functional characterization of pheochromocytoma and paraganglioma by 18F-fluorodeoxyglucose (18F-FDG) positron emission tomography. *J Natl Cancer Inst.* 2012;104:700-708.
32. Amodru V, Guerin C, Delcourt S, et al. Quantitative (18)F-DOPA PET/CT in pheochromocytoma: the relationship between tumor secretion and its biochemical phenotype. *Eur J Nucl Med Mol Imaging.* 2018;45:278-282.
33. Fottner C, Helisch A, Anlauf M, et al. 6-18F-fluoro-L-dihydroxyphenylalanine positron emission tomography is superior to 123I-metaiodobenzyl-guanidine scintigraphy in the detection of extraadrenal and hereditary pheochromocytomas and paragangliomas: correlation with vesicular monoamine transporter expression. *J Clin Endocrinol Metab.* 2010;95:2800-2810.
34. Luster M, Karges W, Zeich K, et al. Clinical value of 18F-fluorodihydroxyphenylalanine positron emission tomography/computed tomography (18F-DOPA PET/CT) for detecting pheochromocytoma. *Eur J Nucl Med Mol Imaging.* 2010;37:484-493.
35. Choyke PL, Glenn GM, Walther MM, Patronas NJ, Linehan WM, Zbar B. von Hippel-Lindau disease: genetic, clinical, and imaging features. *Radiology.* 1995;194:629-642.
36. Richard S, Resche F, Vermeesse B, et al. Pheochromocytoma as Presenting Manifestation of Vonhippellindau Disease. *Archives Des Maladies Du Coeur Et Des Vaisseaux.* 1992;85:1153-1156.
37. Neumann HP, Berger DP, Sigmund G, et al. Pheochromocytomas, multiple endocrine neoplasia type 2, and von Hippel-Lindau disease. *N Engl J Med.* 1993;329:1531-1538.
38. Kaji P, Carrasquillo JA, Linehan WM, et al. The role of 6-[18F]fluorodopamine positron emission tomography in the localization of adrenal pheochromocytoma associated with von Hippel-Lindau syndrome. *Eur J Endocrinol.* 2007;156:483-487.
39. Tiwari A, Shah N, Sarathi V, et al. Genetic status determines (18) F-FDG uptake in pheochromocytoma/paraganglioma. *J Med Imaging Radiat Oncol.* 2017;61:745-752.
40. Srirangalingam U, Khoo B, Walker L, et al. Contrasting clinical manifestations of SDHB and VHL associated chromaffin tumours. *Endocr Relat Cancer.* 2009;16:515-525.
41. Rischke HC, Benz MR, Wild D, et al. Correlation of the genotype of paragangliomas and pheochromocytomas with their metabolic phenotype on 3,4-dihydroxy-6-18F-fluoro-L-phenylalanin PET. *J Nucl Med.* 2012;53:1352-1358.
42. Hoegerle S, Nitzsche E, Altehoefer C, et al. Pheochromocytomas: detection with 18F DOPA whole body PET--initial results. *Radiology.* 2002;222:507-512.

43. Weisbrod AB, Kitano M, Gesuwan K, et al. Clinical utility of functional imaging with (1)(8)F-FDOPA in Von Hippel-Lindau syndrome. *J Clin Endocrinol Metab.* 2012;97:E613-617.
44. Bausch B, Schiavi F, Ni Y, et al. Clinical Characterization of the Pheochromocytoma and Paraganglioma Susceptibility Genes SDHA, TMEM127, MAX, and SDHAF2 for Gene-Informed Prevention. *JAMA Oncol.* 2017;3:1204-1212.
45. Burnichon N, Cascon A, Schiavi F, et al. MAX mutations cause hereditary and sporadic pheochromocytoma and paraganglioma. *Clin Cancer Res.* 2012;18:2828-2837.
46. Taieb D, Jha A, Guerin C, et al. 18F-FDOPA PET/CT Imaging of MAX-Related Pheochromocytoma. *J Clin Endocrinol Metab.* 2018;103:1574-1582.
47. Fishbein L, Merrill S, Fraker DL, Cohen DL, Nathanson KL. Inherited mutations in pheochromocytoma and paraganglioma: why all patients should be offered genetic testing. *Ann Surg Oncol.* 2013;20:1444-1450.
48. Zinamosca L, Petramala L, Cotesta D, et al. Neurofibromatosis type 1 (NF1) and pheochromocytoma: prevalence, clinical and cardiovascular aspects. *Arch Dermatol Res.* 2011;303:317-325.
49. Gruber LM, Erickson D, Babovic-Vuksanovic D, Thompson GB, Young WF, Jr., Bancos I. Pheochromocytoma and paraganglioma in patients with neurofibromatosis type 1. *Clin Endocrinol (Oxf).* 2017;86:141-149.
50. Bausch B, Borozdin W, Neumann HP, European-American Pheochromocytoma Study G. Clinical and genetic characteristics of patients with neurofibromatosis type 1 and pheochromocytoma. *N Engl J Med.* 2006;354:2729-2731.
51. Kepenekian L, Mognetti T, Lifante JC, et al. Interest of systematic screening of pheochromocytoma in patients with neurofibromatosis type 1. *Eur J Endocrinol.* 2016;175:335-344.
52. Zhuang Z, Yang C, Lorenzo F, et al. Somatic HIF2A gain-of-function mutations in paraganglioma with polycythemia. *N Engl J Med.* 2012;367:922-930.
53. Pacak K, Jochmanova I, Prodanov T, et al. New syndrome of paraganglioma and somatostatinoma associated with polycythemia. *J Clin Oncol.* 2013;31:1690-1698.
54. Janssen I, Chen CC, Zhuang Z, et al. Functional Imaging Signature of Patients Presenting with Polycythemia/Paraganglioma Syndromes. *J Nucl Med.* 2017;58:1236-1242.
55. Fishbein L, Nathanson KL. Pheochromocytoma and paraganglioma: understanding the complexities of the genetic background. *Cancer Genet.* 2012;205:1-11.
56. Tufton N, Ghelani R, Srirangalingam U, et al. SDHA mutated paragangliomas may be at high risk of metastasis. *Endocr Relat Cancer.* 2017;24:L43-L49.
57. Jha A, de Luna K, Balili CA, et al. Clinical, Diagnostic, and Treatment Characteristics of SDHA-Related Metastatic Pheochromocytoma and Paraganglioma. *Front Oncol.* 2019;9:53.

- 58.** Timmers HJ, Kozupa A, Chen CC, et al. Superiority of fluorodeoxyglucose positron emission tomography to other functional imaging techniques in the evaluation of metastatic SDHB-associated pheochromocytoma and paraganglioma. *J Clin Oncol.* 2007;25:2262-2269.
- 59.** Zelinka T, Timmers HJ, Kozupa A, et al. Role of positron emission tomography and bone scintigraphy in the evaluation of bone involvement in metastatic pheochromocytoma and paraganglioma: specific implications for succinate dehydrogenase enzyme subunit B gene mutations. *Endocr Relat Cancer.* 2008;15:311-323.
- 60.** Timmers HJ, Chen CC, Carrasquillo JA, et al. Comparison of 18F-fluoro-L-DOPA, 18F-fluoro-deoxyglucose, and 18F-fluorodopamine PET and 123I-MIBG scintigraphy in the localization of pheochromocytoma and paraganglioma. *J Clin Endocrinol Metab.* 2009;94:4757-4767.
- 61.** Gimenez-Roqueplo AP, Caumont-Prim A, Houzard C, et al. Imaging work-up for screening of paraganglioma and pheochromocytoma in SDHx mutation carriers: a multicenter prospective study from the PGL.EVA Investigators. *J Clin Endocrinol Metab.* 2013;98:E162-173.
- 62.** Janssen I, Blanchet EM, Adams K, et al. Superiority of [68Ga]-DOTATATE PET/CT to Other Functional Imaging Modalities in the Localization of SDHB-Associated Metastatic Pheochromocytoma and Paraganglioma. *Clin Cancer Res.* 2015;21:3888-3895.
- 63.** Jha A, Ling A, Millo C, et al. Superiority of (68)Ga-DOTATATE over (18)F-FDG and anatomic imaging in the detection of succinate dehydrogenase mutation (SDHx)-related pheochromocytoma and paraganglioma in the pediatric population. *Eur J Nucl Med Mol Imaging.* 2018;45:787-797.